

















Simulation of power grids using multirate methods

Simulación de redes eléctricas mediante métodos multitasas

Galván-Sánchez, Verónica Adriana^{*a}, Gutiérrez-Robles, José Alberto^b, Bañuelos-Cabral, Eduardo Salvador^c and López de Alba, Carlos Alberto^d^a  Universidad de Guadalajara •  ADT-7409-2022 •  0000-0002-5462-2361 •  293960^b  Universidad de Guadalajara •  LMN-4565-2024 •  0000-0002-0276-0244 •  30264^c  Universidad de Guadalajara •  AAF-2785-2021 •  0000-0002-6004-5898 •  241756^d  Universidad de Guadalajara •  LMN-5894-2024 •  0000-0002-5914-9884 •  256222

CONAHCYT classification:

Area: Engineering

Field: Technological science

Discipline: Energy technology

Subdiscipline: Power transmission

 <https://doi.org/10.35429/JCS.2024.8.19.2.13>

Article History:

Received: January 31, 2024

Accepted: December 31, 2024

* ✉ [\[veronica.galvan@academicos.udg.mx\]](mailto:veronica.galvan@academicos.udg.mx)

Abstract

This article describes a methodology based on Gabriel Kron's diakoptics technique for efficiently simulating an electrical network. The methodology involves dividing a large electrical network into subnetworks that are decoupled in time from each other. For the purpose of network division, it is assumed that the resulting subnetworks are interconnected by transmission lines. The effectiveness of the proposed methodology is demonstrated through an application example in which the transient response of a network is first simulated without partitions, using the high resolution required by the transient phenomenon. Then, the same simulation is performed, but this time with the network divided into two partitions, using the same integration step for both subnetworks. Finally, the two subnetworks are simulated with different integration steps, according to the dynamics of each. The comparison of results and computation times from these three simulations confirms that transient simulations in large networks can be accelerated without compromising the accuracy of the results.

Objetives

Correctly simulate transient state using line models with frequency dependence using an electrical network with two or more modules (subsystems), using multirate techniques, that is, different integration steps for each subsystem. However, for the purposes of exemplifying the methodology, the exchange of information and the sequence of operations, the Bergeron model with losses is used.

Methodology

Methodology based on Gabriel Kron's diakoptics technique to simulate an electrical network. It consists of dividing an electrical network into subnetworks that are decoupled in time from each other. To carry out the division of a network, it is assumed that the resulting subnetworks are joined with transmission lines. The effectiveness of the methodology is demonstrated through an application in which the transient response is simulated without partitioning and with the network divided into two partitions.

Contributions

A methodology is presented to simulate a network separated into blocks. It is shown that there can be reconfigurations in the interconnection of the blocks without the need to recalculate the nodal admittance matrices. The separation, as proposed, is suitable for simulating each block with a different processor and a specific time step. The need for a filtering stage is shown.

Resumen

En este artículo se describe una metodología basada en la técnica de diaópticas de Gabriel Kron para simular eficientemente una red eléctrica. La metodología consiste en la división de una red eléctrica grande en subredes que estén desacopladas en tiempo entre sí. Para efectuar la división de una red aquí se supone que las subredes resultantes se unen entre sí mediante líneas de transmisión. La efectividad de la metodología propuesta se demuestra a través de un ejemplo de aplicación en el cual la respuesta transitoria de una red se simula primero sin particiones y con la alta resolución requerida por el fenómeno transitorio. Después, la misma simulación es efectuada, pero ahora con la red dividida en dos particiones y utilizando el mismo paso de integración para ambas subredes. Finalmente, las dos subredes se simulan con diferentes pasos de integración, de acuerdo con la dinámica de cada una de ellas. La comparación entre resultados y de tiempos de cómputo de estas tres simulaciones confirma que las simulaciones de transitorios en redes de gran tamaño pueden acelerarse sin comprometer la precisión de los resultados.

Objetivos

Simular correctamente estado transitorio utilizando de modelos de línea con dependencia frecuencial utilizando una red eléctrica con dos o más módulos (subsistemas), utilizando técnicas de multitasas, es decir, diferentes pasos de integración para cada subsistema. Sin embargo, para efectos de ejemplificar la metodología, el intercambio de información y la secuencia de operaciones se utiliza el modelo de Bergeron con pérdidas.

Metodología

Metodología basada en la técnica de diaópticas de Gabriel Kron para simular una red eléctrica. Consiste en la división de una red eléctrica en subredes que estén desacopladas en tiempo entre sí. Para efectuar la división de una red se supone que las subredes resultantes se unen con líneas de transmisión. La efectividad de la metodología se demuestra a través de una aplicación en el cual la respuesta transitoria se simula sin partición y con la red dividida en dos partes.

Contribuciones

Se presenta una metodología para simular una red separada en bloques. Se muestra que puede haber reconfiguraciones en la interconexión de los bloques sin necesidad de recalcular las matrices de admitancias nodales. La separación, tal como se propone, es adecuada para simular cada bloque con un procesador diferente y un paso de tiempo específico. Se muestra la necesidad de una etapa de filtrado.

Bergeron, EMTP, Multirate

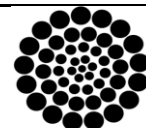
Bergeron, EMTP, Multitasas

Citation: Galván-Sánchez, Verónica Adriana, Gutiérrez-Robles, José Alberto, Bañuelos-Cabral, Eduardo Salvador and López de Alba, Carlos Alberto. [2024]. Simulation of power grids using multirate methods. Journal Computational Simulation. 8[19]-1-13: e20819113.



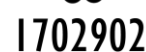
ISSN 2523-6865/© 2009 The Author[s]. Published by ECORFAN-Mexico, S.C. for its Holding Taiwan on behalf of Journal Computational Simulation. This is an open access article under the CC BY-NC-ND license [<http://creativecommons.org/licenses/by-nc-nd/4.0/>]

Peer Review under the responsibility of the Scientific Committee MARVID®. in contribution to the scientific, technological and innovation Peer Review Process by training Human Resources for the continuity in the Critical Analysis of International Research.



RENECYT

Registro Nacional de Instituciones y Empresas Científicas y Tecnológicas



1702902 CONAHCYT

Introduction

In recent years, electrical power systems have shown a sustained increase in the complexity of their analysis processes. This is a consequence of several factors, among which stands out the constant increase in the dimensions of the systems due to the inclusion of new generating stations, substations, etc.; this makes the simulation of such systems more and more demanding from the computational point of view. In addition, the models used to represent the elements of a network add considerable computational and computational memory requirements. All this, added to the need to offer better quality services, means that the simulation programs traditionally used in the study of various phenomena and events involved in the operation of these systems require the implementation of new technological platforms that allow obtaining results at a higher speed. In this context, real-time simulation stands out in particular.

In most cases, a disturbance of a large electrical network only causes a small part of it to enter into fast dynamic operation, while the majority of the network will remain in a slow dynamic state. The difference in response time makes it possible to split the network and simulate each of the resulting blocks with different time steps. Thus, it is convenient to use large integration steps for subnetworks with slow dynamics, while small integration steps are reserved for subnetworks operating with fast dynamics. This technique, which is known as multirate, provides large increases in the computational efficiency of dynamic simulations; however, the state variables that are exchanged between subnetwork models running with different integration steps must be conditioned. Signals coming from a submodule with fast dynamics, going to one with slower dynamics, must first be passed through a low-pass filter and then decimated.

This is in order to avoid aliasing errors. On the other hand, signals coming from a submodule with slow dynamics, and going to one with faster dynamics, must first be interpolated and then passed through a low-pass filter that eliminates errors due to spurious spectral components produced by the interpolation.

Historical background

In the 1950s, in order to simulate large networks, Gabriel Kron developed a network partitioning technique that he called Diacopectics (Kron G. 1-7). However, the use of this technique did not become universal, and it was not until the 1970s when Happ et. al. took up the development of G. Kron for the solution and analysis of power systems (Happ, H. H.).

In 1975, Ho et. al. published a paper on Modified Nodal Analysis (MNA) (Chung-Wen H. et.al.). MNA separates the solution of a network into nodal and branch equations, and although the authors do not relate their work to the diacopectic techniques, the equations resulting from MNA are the same as those resulting from G. Kron's techniques.

In the 1990s, in the search to increase the simulation speed, A. Semlyen presents a procedure to calculate electromagnetic transients using two or more time steps (Semlyen, A. & De Leon, F.). He makes a distinction to fast buses, which he simulates with a smaller time step than the rest of the network. He proposes the coupling of variables through a line-bus interface based on traveling waves and implements the interface by interpolating the incident wave and smoothing the reflected wave. In turn, J. R. Martí extends the ideas of diacopectic techniques in the MATE (Multi Area Thevenin Equivalent) concept, which subdivides the system into independent sub-networks, except for the links that unite them (Martí, J. R. et.al. (1)).

Proposed methodology

The proposed method consists of the application of G. Kron's diacopectic techniques (Kron G. 1-7) to separate a network into subsystems interconnected by transmission lines. The models of the network elements are those used in EMTP; however, this method differs from the traditional methodology used in EMTP in that when doing the network separation, each subsystem is resolved as if the tie lines did not exist, and then the voltages of the subsystems are updated using information from the existing interconnections.

The modeling of transmission lines in time domain is traditionally done with two-port EMTP type models, such as the Bergeron model (Dommel, H. W.), the J. Marti model (Marti, J. R. (3)), the universal model (Morched, A. et.al.) or the model based on the method of characteristics (Naredo J. L. et.al. (1)); all models have in common the schematic form. Figure 1 shows Bergeron's model, as used in EMTP, where it is illustrated for a line connected between nodes k and m. In this figure, I_{km} and I_{mk} are the outgoing currents of those nodes, h_{km} and h_{mk} are the associated history currents, V_m and V_k are the voltages at the nodes and Z_C is the characteristic impedance of the line (Dommel, H. W.). Additional elements that interconnect in a network, such as inductance, capacitance and resistance, have similar models (Dommel, H. W.).

Box 1

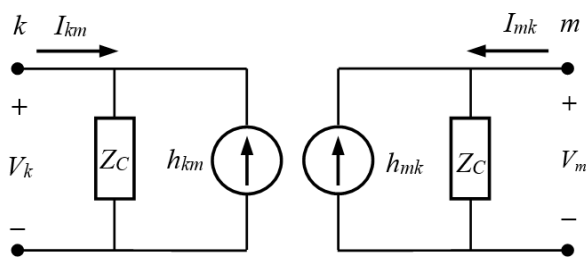


Figure 1

Diagram of the solution of the line with the Bergeron model

Source: Own elaboration

According to the schematic in figure 1, it can be seen that the lines decouple the network, so that subsystems can be formed in a natural way separated by transmission lines. This allows the parallel execution of the network, but with the following limitation: if you want to make a change during the simulation in the network topology by inserting or removing lines between two subsystems, you need to modify the nodal admittance matrix, which increases the solution time considerably. The method proposed here, in addition to the time reduction by simulation using subsystems, solves the dynamic reconfiguration problem satisfactorily.

The network in figure 2 is used to derive the method. The separation of the network is done in the line from node 2 to node 3; figure 3 shows how the partitioned network looks like, where it is also observed the reassignment in the numbering of the nodes as if each subsystem was independent.

Box 2

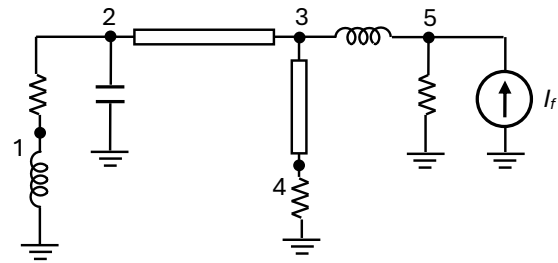


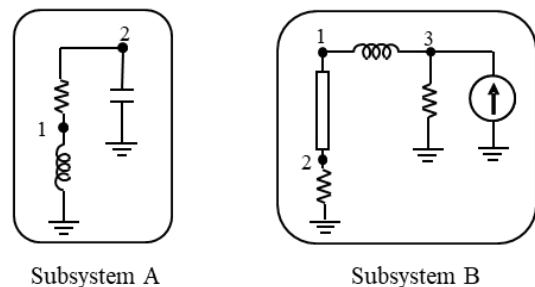
Figure 2

Test network

Source: Own elaboration

Figure 3 shows that, regardless of the number of interconnections between subsystems, the nodal admittance matrix of each subsystem does not change; in this way, the links between subsystems can be reconfigured without changing the equations that give solutions to the internal voltages of each subsystem; thus, only the updates due to the interconnections between them are modified. The derivation of the proposed method is presented in detail below.

Box 3



Subsystem A

Subsystem B

Figure 3

Network separation scheme in Figure 2.

Own figure

The nodal equations of each subsystem as an independent network are expressed as follows:

$$\begin{aligned} [\mathbf{A}][\mathbf{V}_A] &= [\mathbf{H}_A] \\ [\mathbf{B}][\mathbf{V}_B] &= [\mathbf{H}_B] \end{aligned} \quad [1]$$

where y are the nodal admittance matrices of each sub-network, y are the nodal voltage vectors, and y are vectors containing the sources of each network and the current histories due to the solution method (Dommel, H. W.).

If the set of equations (1) is grouped into a single matrix system, the following is obtained.

$$\begin{bmatrix} \mathbf{A} & \mathbf{0} \\ \mathbf{0} & \mathbf{B} \end{bmatrix} \begin{bmatrix} \mathbf{V}_A \\ \mathbf{V}_B \end{bmatrix} = \begin{bmatrix} \mathbf{H}_A \\ \mathbf{H}_B \end{bmatrix}, \quad [2]$$

If the submatrices are expanded according to figure 3, the following system of equations is obtained:

$$\begin{bmatrix} Y_{A,11} & Y_{A,12} & 0 & 0 & 0 \\ Y_{A,21} & Y_{A,22} & 0 & 0 & 0 \\ 0 & 0 & Y_{B,11} & Y_{B,12} & Y_{B,13} \\ 0 & 0 & Y_{B,21} & Y_{B,22} & Y_{B,23} \\ 0 & 0 & Y_{B,31} & Y_{B,32} & Y_{B,33} \end{bmatrix} \begin{bmatrix} v_{A1} \\ v_{A2} \\ v_{B1} \\ v_{B2} \\ v_{B3} \end{bmatrix} = \begin{bmatrix} H_{A1} \\ H_{A2} \\ H_{B1} \\ H_{B2} \\ H_{B3} \end{bmatrix}, \quad [3]$$

In equation (3) and thereafter, the notation used is as follows: Y is admittance, the subscripts A, B, and the numbering designate the module or block to which a parameter belongs and specifically the nodes to which it is associated. This equation clearly shows how up to this point the interconnection line has not been taken into account in the construction of the nodal admittance matrix.

In order to take the tie line into account without modifying the nodal admittance matrix, it is modelled as outgoing current sources from the interconnection nodes, as can be seen in Figure 4. In this figure and in the following, the subscripts L1 indicate relationship to tie line 1; the subscripts AB and BA indicate that the current goes from subsystem A to B and vice versa; ZL1 is the characteristic impedance of tie line 1.

Box 4

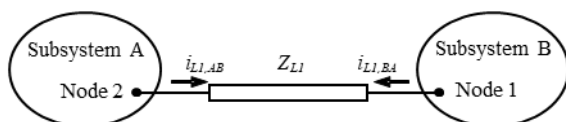


Figure 4

Interconnection diagram between subsystems

Source: Own elaboration

Thus, adding the junction line currents, $iL_{1,AB}$ and $iL_{1,BA}$, from equation (3) gives the new system of equations.

$$\begin{bmatrix} Y_{A,11} & Y_{A,12} & 0 & 0 & 0 & 0 & 0 \\ Y_{A,21} & Y_{A,22} & 0 & 0 & 0 & 1 & 0 \\ 0 & 0 & Y_{B,11} & Y_{B,12} & Y_{B,13} & 0 & 1 \\ 0 & 0 & Y_{B,21} & Y_{B,22} & Y_{B,23} & 0 & 0 \\ 0 & 0 & Y_{B,31} & Y_{B,32} & Y_{B,33} & 0 & 0 \\ 0 & 0 & 0 & 0 & 0 & -Z_{L1} & 0 \\ 0 & 0 & 0 & 0 & 0 & 0 & -Z_{L1} \end{bmatrix} \begin{bmatrix} v_{A1} \\ v_{A2} \\ v_{B1} \\ v_{B2} \\ v_{B3} \\ i_{L1,AB} \\ i_{L1,BA} \end{bmatrix} = \begin{bmatrix} H_{A1} \\ H_{A2} \\ H_{B1} \\ H_{B2} \\ H_{B3} \\ H_{L1,AB} \\ H_{L1,BA} \end{bmatrix}, \quad [4]$$

The system of equations given by (4) is underdetermined, so to form a system of equations with a unique solution we use the equations of the connecting line, which are:

$$i_{L1,AB}(t) = \frac{1}{Z_{L1}} v_{A2}(t) + h_{L1,AB}(t), \quad [5a]$$

$$i_{L1,BA}(t) = \frac{1}{Z_{L1}} v_{B1}(t) + h_{L1,BA}(t), \quad [5b]$$

Where $h_{L1,AB}$ y $h_{L1,BA}$ are currents of history (Dommel, H. W.).

In order to incorporate equations (5) into (4), they are first multiplied by the characteristic impedance of the line, and after an algebraic rearrangement we obtain

$$v_{A2}(t) - Z_{L1} i_{L1,AB}(t) = H_{L1,AB}(t), \quad [6a]$$

$$v_{B1}(t) - Z_{L1} i_{L1,BA}(t) = H_{L1,BA}(t), \quad [6b]$$

where the terms H_{L1} are history voltages, which are given by the following equations for a time t and a travel time of the line τ :

$$H_{L1,AB}(t) = v_{B1}(t - \tau) + Z_{L1} i_{L1,BA}(t - \tau), \quad [7a]$$

$$H_{L1,BA}(t) = v_{A2}(t - \tau) - Z_{L1} i_{L1,AB}(t - \tau) \quad [7b]$$

Equations (6) are integrated into the matrix system given by (4) to obtain

$$\begin{bmatrix} Y_{A,11} & Y_{A,12} & 0 & 0 & 0 & 0 & 0 \\ Y_{A,21} & Y_{A,22} & 0 & 0 & 0 & 1 & 0 \\ 0 & 0 & Y_{B,11} & Y_{B,12} & Y_{B,13} & 0 & 1 \\ 0 & 0 & Y_{B,21} & Y_{B,22} & Y_{B,23} & 0 & 0 \\ 0 & 0 & Y_{B,31} & Y_{B,32} & Y_{B,33} & 0 & 0 \\ 0 & 1 & 0 & 0 & 0 & -Z_{L1} & 0 \\ 0 & 0 & 1 & 0 & 0 & 0 & -Z_{L1} \end{bmatrix} \begin{bmatrix} v_{A1} \\ v_{A2} \\ v_{B1} \\ v_{B2} \\ v_{B3} \\ i_{L1,AB} \\ i_{L1,BA} \end{bmatrix} = \begin{bmatrix} H_{A1} \\ H_{A2} \\ H_{B1} \\ H_{B2} \\ H_{B3} \\ H_{L1,AB} \\ H_{L1,BA} \end{bmatrix}, \quad [8]$$

A matrix partition is made in equation (8), but the following matrices are assigned first:

$$\mathbf{U}_B = \begin{bmatrix} 0 & 1 \\ 0 & 0 \\ 0 & 0 \end{bmatrix} \quad [9a]$$

$$\mathbf{Z}_L = \begin{bmatrix} -Z_{L1} & 0 \\ 0 & -Z_{L1} \end{bmatrix} \quad [9b]$$

$$\mathbf{I}_L = \begin{bmatrix} i_{L1,AB} \\ i_{L1,BA} \end{bmatrix} \quad [9c]$$

$$\mathbf{H}_A = \begin{bmatrix} H_{A1} \\ H_{A2} \end{bmatrix}, \mathbf{H}_B = \begin{bmatrix} H_{B1} \\ H_{B2} \\ H_{B3} \end{bmatrix}, \mathbf{H}_L = \begin{bmatrix} H_{L1,AB} \\ H_{L1,BA} \end{bmatrix} \quad [9d]$$

Using the matrix notation given by (9), we obtain in compact form

$$\begin{bmatrix} \mathbf{A} & \mathbf{0} & \mathbf{U}_A \\ \mathbf{0} & \mathbf{B} & \mathbf{U}_B \\ \mathbf{U}_A^T & \mathbf{U}_B^T & \mathbf{Z}_L \end{bmatrix} \begin{bmatrix} \mathbf{V}_A \\ \mathbf{V}_B \\ \mathbf{I}_L \end{bmatrix} = \begin{bmatrix} \mathbf{H}_A \\ \mathbf{H}_B \\ \mathbf{H}_L \end{bmatrix} \quad [10]$$

If we pre-multiply the system of equations (10) by

$$\begin{bmatrix} \mathbf{A}^{-1} & 0 & 0 \\ 0 & \mathbf{B}^{-1} & 0 \\ 0 & 0 & \mathbf{U} \end{bmatrix}, \quad [11]$$

with equal to a unitary matrix of the corresponding dimension, we get

$$\begin{bmatrix} \mathbf{U} & 0 & \mathbf{A}^{-1}\mathbf{U}_A \\ 0 & \mathbf{U} & \mathbf{B}^{-1}\mathbf{U}_B \\ \mathbf{U}_A^T & \mathbf{U}_B^T & \mathbf{Z}_L \end{bmatrix} \begin{bmatrix} \mathbf{V}_A \\ \mathbf{V}_B \\ \mathbf{I}_L \end{bmatrix} = \begin{bmatrix} \mathbf{A}^{-1}\mathbf{H}_A \\ \mathbf{B}^{-1}\mathbf{H}_B \\ \mathbf{H}_L \end{bmatrix} \quad [12]$$

From the system of equations (12) we extract and , which are given as follows

$$\mathbf{V}_A = \mathbf{A}^{-1}\mathbf{H}_A - \mathbf{A}^{-1}\mathbf{U}_A\mathbf{I}_L \quad [13a]$$

$$\mathbf{V}_B = \mathbf{B}^{-1}\mathbf{H}_B - \mathbf{B}^{-1}\mathbf{U}_B\mathbf{I}_L \quad [13b]$$

A comparison of the first term on the right-hand side of equation (13) with the solution of equation (1) shows that they are equivalent and relate to the solution of each subsystem independently. Thus, if the vectors \mathbf{E} are defined as

$$\mathbf{E}_A = \mathbf{A}^{-1}\mathbf{H}_A, \quad [14a]$$

$$\mathbf{E}_B = \mathbf{B}^{-1}\mathbf{H}_B, \quad [14b]$$

then equation (13) can be written in the following way:

$$\mathbf{V}_A = \mathbf{E}_A - \mathbf{A}^{-1}\mathbf{U}_A\mathbf{I}_L \quad [15a]$$

$$\mathbf{V}_B = \mathbf{E}_B - \mathbf{B}^{-1}\mathbf{U}_B\mathbf{I}_L \quad [15b]$$

Equations (15) can be interpreted as follows:

1. First, the nodal voltages of the two sub-networks are calculated separately.

2. With the current flowing through the tie line, the nodal voltages are modified to obtain the actual voltage of the interconnected subsystems.

Since the calculation of the nodal voltages of the complete network requires the current flowing through the tie line, from the system of equations given by (12) we obtain:

$$\mathbf{I}_L = \mathbf{Z}_L^{-1} \left[\mathbf{H}_L - \mathbf{U}_A^T \mathbf{V}_A - \mathbf{U}_B^T \mathbf{V}_B \right] \quad [16a]$$

Substitute equations (15) into (16a) and get

$$\mathbf{I}_L = \mathbf{Z}_L^{-1} \mathbf{H}_L - \mathbf{Z}_L^{-1} \mathbf{U}_A^T (\mathbf{E}_A - \mathbf{A}^{-1} \mathbf{U}_A \mathbf{I}_L) - \mathbf{Z}_L^{-1} \mathbf{U}_B^T (\mathbf{E}_B - \mathbf{B}^{-1} \mathbf{U}_B \mathbf{I}_L) \quad [16b]$$

After some algebraic manipulations and the introduction of the definition of the constant as

$$\mathbf{K} = \left[\mathbf{U} - \mathbf{Z}_L^{-1} (\mathbf{U}_A^T \mathbf{A}^{-1} \mathbf{U}_A + \mathbf{U}_B^T \mathbf{B}^{-1} \mathbf{U}_B) \right]^{-1} \mathbf{Z}_L^{-1}, \quad [17]$$

the expression is arrived at as follows,

$$\mathbf{I}_L = \mathbf{K} (\mathbf{H}_L - \mathbf{U}_A^T \mathbf{E}_A - \mathbf{U}_B^T \mathbf{E}_B), \quad [18]$$

where the term is a 2x2 diagonal matrix and the term in parentheses, in extended form, is

$$\mathbf{H}_L - \mathbf{U}_A^T \mathbf{E}_A - \mathbf{U}_B^T \mathbf{E}_B = \begin{bmatrix} H_{L1,AB} \\ H_{L1,BA} \end{bmatrix} - \begin{bmatrix} E_{A2} \\ 0 \end{bmatrix} - \begin{bmatrix} 0 \\ E_{B1} \end{bmatrix} \quad [19]$$

Substituting (17) and (19) into (18) we get

$$\begin{bmatrix} I_{L1,AB} \\ I_{L1,BA} \end{bmatrix} = \begin{bmatrix} \mathbf{K}_{11} & 0 \\ 0 & \mathbf{K}_{22} \end{bmatrix} \begin{bmatrix} H_{L1,AB} - E_{A2} \\ H_{L1,BA} - E_{B1} \end{bmatrix}. \quad [20]$$

Thus, we finally arrive at the current equations in the link line

$$i_{L1,AB}(t) = \mathbf{K}_{11} (H_{L1,AB}(t) - E_{A2}(t)) \quad [20a]$$

$$i_{L1,BA}(t) = \mathbf{K}_{22} (H_{L1,BA}(t) - E_{B1}(t)) \quad [20b]$$

Equation (20) shows that the current at each end of the line depends on the internal voltage of the networks at the junction point as if the interconnection did not exist and on the history voltage of the junction line.

This leaves the equations needed to simulate a network using parallel processing. The flowchart indicating the order and operations required for the network simulation is presented below.

Multirate transients

In an electrical network, not all elements respond at the same rate; for example, there are occasions when two regions can be distinguished: one region with a fast disturbance and another that operates close to steady state. It is in such situations that the network can be conveniently divided for analysis into two regions; such is the case of the test network illustrated in figure 2, whose separation by the proposed method is shown in figure 3. Once the network is separated and the sectors with fast and slow dynamics are identified, simulation with different time steps for each sector becomes possible.

The interconnection between the subsystems is done through the transmission line link, and specifically through the voltage histories that in the proposed method are named HLL_{AB} and HLL_{BA} . The former transmits the necessary information from the fast system to the slow system and the latter provides this information from the slow dynamic system to the fast dynamic system. As the systems have different sampling rates, the information exchanged between subsystems must be conditioned; how this is done is described below.

Multirate theory

The process of converting a signal of a given rate to a different rate is called sampling rate conversion.

Systems employing multiple sampling rates in digital signal processing are called multi-rate digital processing systems (Naredo, J. L. et.al. (2)) and (Vaidyanathan, P. P.). Sample rate conversion in the digital domain is performed under the concept of interpolation and decimation.

Decimation. Decimation is characterised by the input-output relationship

$$y_D(n) = x(Mn) \quad [22]$$

This equation, (22), indicates that the output y_D at time n is equal to the input x at time Mn . As a consequence, only input samples with sample numbers equal to a multiple of M are retained. When the input $x(n)$ is undersampled by an integer factor M , the sampling frequency is reduced by selecting every M values of $x(n)$, so the resulting signal is an aliased version of $x(n)$, with an overlapping frequency, where is the maximum frequency of the input signal $x(n)$. To avoid aliasing, the bandwidth of $x(n)$ must first be reduced to a maximum frequency, or equivalently, to $\frac{1}{2M}$. For this task, the sequence $x(n)$ is passed through a low pass filter to remove the spectrum of $x(n)$, ω , in the range $\frac{\pi}{2M} < \omega < \pi$.

Interpolation. An interpolator is characterised by the input-output relation

$$y_I(n) = \begin{cases} x(n/L) & \text{Si } n \text{ es un múltiplo de } L \\ 0 & \text{En otro caso} \end{cases} \quad [23]$$

This means that the interpolated output is obtained by inserting $L-1$ zero-valued samples between adjacent samples of the input $x(n)$. This type of interpolation preserves the spectral shape of the signal $x(n)$. When $L-1$ new samples are interpolated between successive values of the signal, an increase in the sampling frequency is achieved; this results in a signal whose spectrum is a periodic and overlapping repetition L times of the spectrum, which belongs to the input signal. Since the frequency components of $y_I(n)$ in the range $\frac{\pi}{2M} < \omega < \pi$ are unique, the images of above must be removed by passing the sequence $y_I(n)$ through a low-pass filter. Figure 5 shows a one-channel multirate system, showing the decimation and interpolation processes with their respective filters as described above.

Box 5

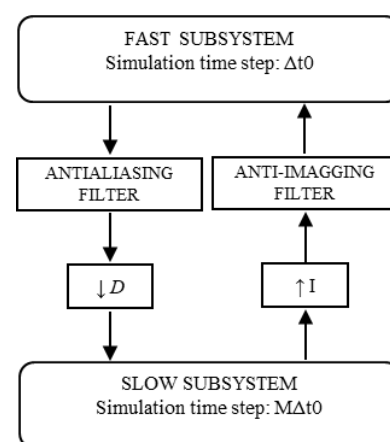


Figure 5

Single-channel multirate system

Source: Own elaboration

Application of the methodology

The proposed method is applied to the test network in figure 2 to perform a qualitative and quantitative analysis on the behaviour of the nodal voltages over time. A detailed description of this network is given below, followed by a description of the stages of this work.

Description of the test system

Table 1 presents the data corresponding to the elements of the test network, as well as their connectivity. The line model is Bergeron with losses concentrated at the ends. The characteristic impedance of the lines is 450Ω and their resistance is 1Ω at each end. In order to maximise the transient state of the network, a cosine function of unit amplitude is used for the current source (at energisation time, $t=0$, the maximum value of the source is presented).

Box 6

Table 1

Connectivity and test case parameters

Source node	Node destination	Element	Value
1	0	Inductance	$25\mu\text{H}$
1	2	Resistance	1Ω
2	0	Capacitance	$1\mu\text{F}$
2	3	Line	150km
3	4	Line	210km
3	5	Inductance	25mH
4	0	Resistance	1Ω
5	0	Resistance	1Ω

The base simulation has a time step $\Delta t_0=0.41667\mu\text{s}$, which corresponds to a travel time of 125m at the speed of light. In all simulation cases, the observation time is 30ms , equivalent to almost 2 cycles of 60Hz .

Description of the stages

In stage 1, the network simulations correspond to the original system (see figure 2), and to the split network as shown in figure 6. In this stage it is satisfied that $N=M$, i.e. the time step in both blocks is the same.

Box 7

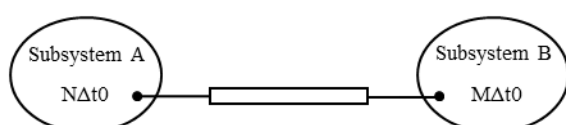


Figure 6

Simulation scheme for the network partitioned into 2 blocks

Source: Own elaboration

The second stage concerns the multi-rate simulations, where the scheme in figure 7 is used with $N=1$, meaning that the base time step is maintained in subsystem A.

Both stages are described in more detail in the following subsections. It should be noted that the error plots included therein refer to the absolute value of the difference between the voltage of a certain node of the base simulation and that of the simulation in question, referenced to the corresponding peak voltage of the base simulation, in percent.

Step 1

Simulations of the original system (figure 2) and the partitioned system are performed with time step variations: from the base, Δt_0 , to $300\Delta t_0$; note that the same time step is used in both blocks. In this part, it is first verified that the separation of a network into blocks yields the same results in the simulation as the originating network, which is true regardless of the time step used. Subsequently, an analysis of the simulation runtimes of the two system configurations is performed: the original system and the system split into two blocks. Table 2 shows the results of the simulation run times for each case. Columns four and five show the reductions, in percent, in the simulation time of the original and block networks, when taking as a reference the execution time of the base system (with Δt_0).

Box 8

Table 2

Simulation times

M	Simulation time (pu)		Reduction of simulation time (%)	
	Red original	Red en bloques	Red original	Red en bloques
1	1	0.233037	0.0000	76.6962
2	0.242621	0.057707	75.7379	94.2292
4	0.059530	0.014662	94.0470	98.5338
6	0.026320	0.006491	97.3679	99.3509
8	0.014621	0.003834	98.5379	99.6165
10	0.009150	0.002320	99.0850	99.7679
12	0.006194	0.001496	99.3806	99.8503
20	0.002083	0.000516	99.7916	99.9484
30	0.000963	0.000239	99.9036	99.9761
40	0.000501	0.000155	99.9498	99.9844
50	0.000316	0.000060	99.9683	99.9940
60	0.000211	0.000046	99.9789	99.9954
100	0.000057	0.000025	99.9942	99.9975
120	0.000031	0.000020	99.9968	99.9979
150	0.000023	0.000018	99.9976	99.9981
200	0.000016	0.000013	99.9983	99.9987
300	0.000009	0.000013	99.9989	99.9991

Table 2 clearly illustrates how from a certain time increment onwards, the simulation times of the block network and the original network are very similar; this is because the communication time between blocks within the observation period for small time steps is irrelevant, but when they increase (M increases) it becomes important.

Figure 7 shows graphically how the reduction of the simulation time of the block network approaches the reduction of the original network as the time step increases; in other words, the block network starts to require the same simulation time as the full network.

Box 9

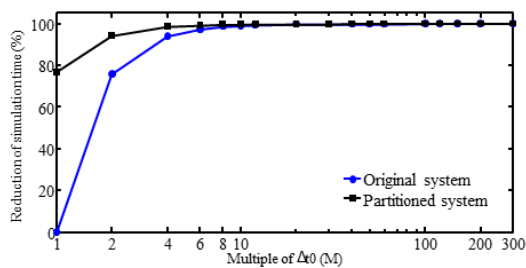


Figure 7

Reduction of simulation time compared to the base simulation

Source: Own elaboration

Regarding the errors related to the time step used, figure 8 shows the maximum errors obtained over the whole time. The error at node 5 is omitted as it is negligible compared to the rest, due to the fact that the source is connected to it.

Figure 9 presents the steady-state errors in the voltages. This figure shows how the errors are substantially reduced to less than 0.1%, except for node 1, where an inductance is connected.

Figure 10 presents the behaviour of the error from the beginning of the simulation until it stabilises; the errors of all simulations (all M) are presented. Only node 1 is presented, as the behaviour is similar for the rest of the nodes. It can be seen in this figure the gradual decrease of the error, independently of the time step. For this purpose, a close-up of the first oscillation and the steady state is presented.

Box 10

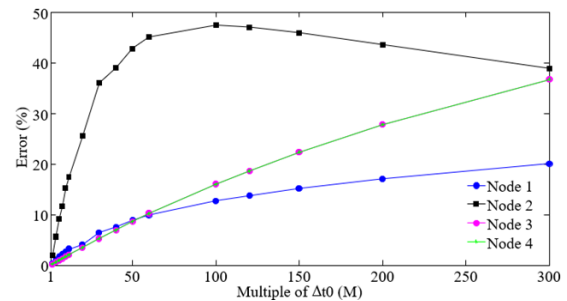


Figure 8

Maximum errors in nodal voltages

Source: Own elaboration

Box 11

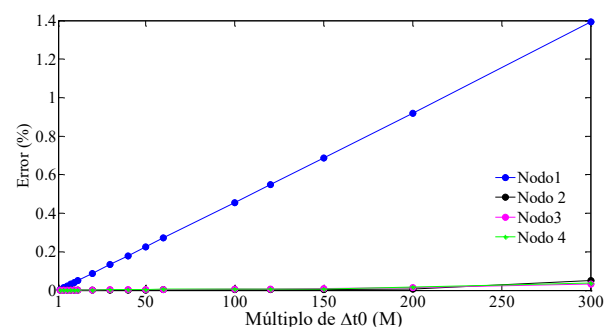


Figure 9

Minimum errors (during steady state) in nodal voltages

Source: Own elaboration

Box 12

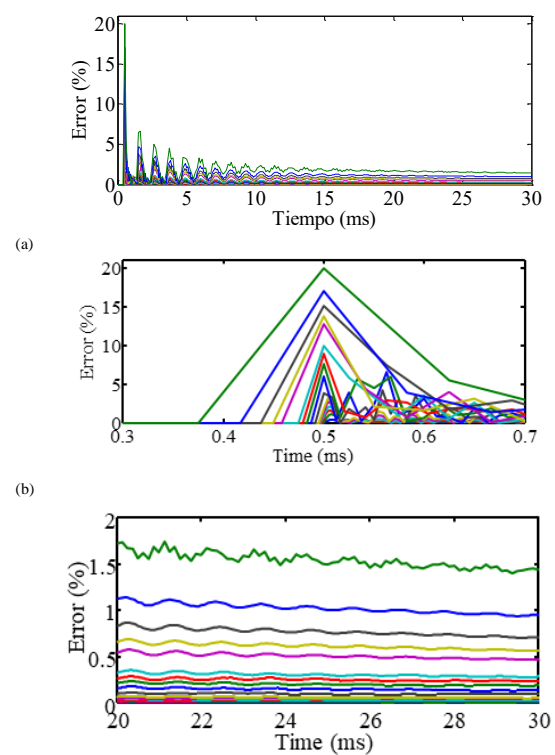


Figure 10

Voltage error throughout the simulation at node 1. (a) Full simulation. (b) Approach to maximum error. (c) Approach to minimum error

Source: Own elaboration

At this stage, it is concluded that there comes a point where the time savings due to the use of several processors is not significant when simulating a block-partitioned power system.

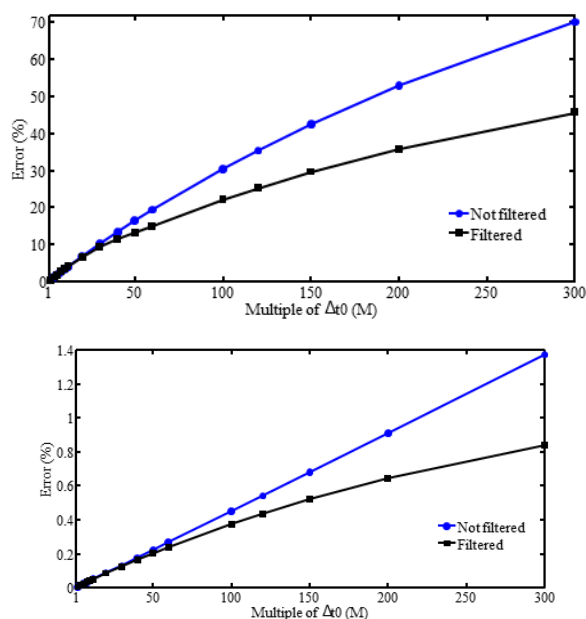
Also, according to the results obtained, it can be said that the use of relatively large time increments can be adequate to simulate steady state, although it yields large errors in transient state.

Stage 2

In this stage, the test network is simulated with multi-rate, as shown in Figure 5. In subsystem A, the base time step, Δt_0 , is always used, while in subsystem B, $M\Delta t_0$ is used, and M is varied from 2 to 300.

The first test is to verify the influence of the filtering stage on the errors of the nodal voltages of the signals exchanged between subsystems. Figure 11 shows the maximum and minimum errors at node 1 when the filtering stage is used and when it is omitted.

Box 13



(b)

Figure 11

Errors in node 1 voltages. (a) Maximum errors. (b) Minimum errors

Source: Own elaboration

To verify the qualitative effect of the filtering stage, a comparison of the voltage waveforms at node 2 obtained when using $100\Delta t_0$ in subsystem B is shown in figure 13.

It should be noted that in this case a rectangular window is used for filtering. In figure 13 it can be seen how the filtering steps lead to a better solution from a qualitative point of view. This is why the filtering stages are incorporated and the simulations are carried out.

Box 14

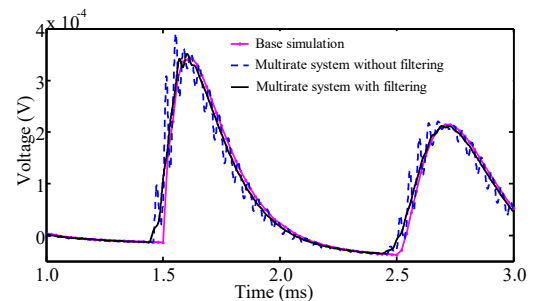


Figure 12

Voltage waveforms at node 2. Base system and multi-rate system with $M = 100$

Figure 13 shows the voltage behaviour at node 2, which belongs to the fast simulation block, for three situations: base simulation (original system with Δt_0), the block system ($M\Delta t_0$ in both subsystems), and the multi-rate system (Δt_0 in subsystem A and $M\Delta t_0$ in subsystem B) with $M=50$. It can be seen how the simulation of the block system does not correctly reproduce the transient state of the fast subsystem, i.e. the M used is no longer adequate to simulate this subsystem.

Box 15

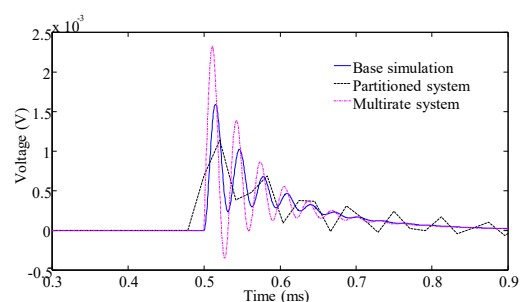


Figure 13

Node 2 voltage waveforms. Base system, block and multi-rate systems

Source: Own elaboration

If only the maximum errors are considered, in apparent form the block system yields better results than if the multiresolution technique is used, as can be seen by comparing figure 14 with figure 8.

However, figure 14 makes it clear that the waveform using multiresolution is more appropriate, as it looks more like the base simulation, the accumulated error during the simulation is lower.

In relation to the steady state, which is where the minimum errors are obtained, the comparison between figures 9 and 15 shows how the use of multiresolution provides a lower error compared to the use of the same time step in both subsystems, which is an expected result.

Box 16

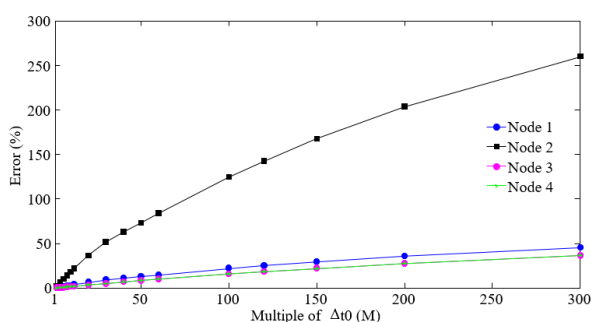


Figure 14

Maximum errors in nodal voltages. Own figure

Box 17

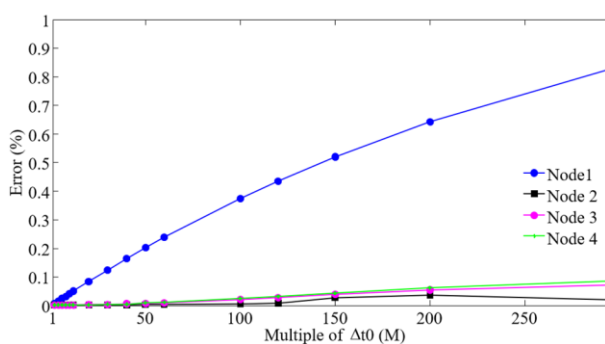


Figure 15

Minimum errors in nodal voltages

Source: Own elaboration

On the other hand, figure 17 shows the results of the reduction in simulation time when going from the base system to the multi-rate system. It can be seen that after a certain time step, the execution time of the simulations is no longer reduced; this is due to the fact that the time taken to exchange information becomes more significant as the simulation time decreases, which in turn is a consequence of increasing the time step in the slow subsystem. Of course, this specific behaviour is specific to this system and its partitioning set-up.

Box 18

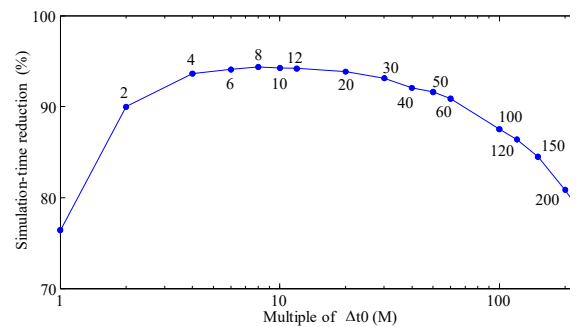


Figure 16

Reduction of simulation time by increasing the time step in subsystem B

Source: Own elaboration

From figure 16 it can also be seen that multirate simulations with M greater than 8 are not useful, since from this M onwards the simulation time does not reduce any further, while the errors continue to increase, as can be seen in figures 14 and 15.

Conclusions

This paper presents a methodology for simulating a network separated into blocks. The methodology shows that there can be reconfigurations in the interconnection of the blocks without the need to recalculate the nodal admittance matrices. The separation, as proposed, is suitable for simulating each block with a different processor and a specific time step; the work shows in detail the equations that model each block and the interconnections between them. To clarify the process, a flow diagram is provided, useful to reproduce the simulations.

To correctly simulate transient state it is necessary to use line models with frequency dependence; however, for the purpose of exemplifying the methodology, the exchange of information and the sequence of operations, the Bergeron model with losses is used.

Furthermore, this work shows the need for a filtering stage and how not just any time step can be used in the slow system, since at a certain point in time, in addition to the increase of the error in the network parameters, the time in which the system is simulated also increases.

It should be clear that the appropriate time steps to simulate each subsystem as well as the way to perform the block separations are specific to each network; this has been extensively studied (Linares, L. R. & Martí, J. R.) and (Moreira, F. A. (3) & Martí, J. R.). and is not the subject of this work.

Conflict of interest

The authors declare that they have no conflicts of interest. They have no known competing financial interests or personal relationships that might have appeared to influence the article reported in this paper.

Authors' contribution

Galván-Sánchez, V. A.: Wrote the article.

Gutiérrez-Robles, J. A.: Development of the simulations and elaboration of the figures in the article.

Bañuelos-Cabral, E. S.: Review, generation and selection of the examples and/or results presented in the article.

López-DeAlba, C. A.: Revision of the content and formatting of the article.

Availability of data and materials

All the results obtained are in the article and are freely available according to the journal's policies.

Funding

The cost of publishing this work in the journal is absorbed by the Universidad de Guadalajara.

Acknowledgements

We are grateful to the University of Guadalajara for funding the publication of this work in the journal.

Abbreviations

MNA Modified Nodal Analysis

EMTP Electromagnetic Transient Programme

MATE Multi-area Thevenin Equivalent

References

Background

Kron, G. (1). [Un método para resolver sistemas físicos muy grandes en etapas fáciles](#). Proceedings of the IRE 42.4, 1954, pp. 680-686. Doi: [10.1109/JRPROC.1954.274704](https://doi.org/10.1109/JRPROC.1954.274704)

Kron, G. (2). [Circuito equivalente de las ecuaciones de campo de Maxwell-I](#). Proceedings of the IRE 32.5, 1944. Doi: [10.1109/JRPROC.1944.231021](https://doi.org/10.1109/JRPROC.1944.231021)

Kron, G. (3). [Un conjunto de principios para interconectar las soluciones de los sistemas físicos](#). Journal of Applied Physics 24.8, 1953, p. 965-980. <https://doi.org/10.1063/1.1721447>

Kron, G. (4). [Tensorial Analysis of Integrated Transmission Systems Part I. The Six Basic Reference Frames](#). American Institute of Electrical Engineers, Transactions of the 70.2, 1951. Doi: [10.1109/T-AIEE.1951.5060553](https://doi.org/10.1109/T-AIEE.1951.5060553)

Kron, G. (5). [Tensorial Analysis of Integrated Transmission Systems; Part II. Off-Nominal Turn Ratios](#). Power Apparatus and Systems, Parte III. Transactions of the American Institute of Electrical Engineers 71.1, 1952, pp. 505-512. Doi: [10.1109/AIEEPAS.1952.4498501](https://doi.org/10.1109/AIEEPAS.1952.4498501)

Kron, G. (6). [Tensorial Analysis of Integrated Transmission Systems, Part III. The Power Apparatus and Systems](#). Transactions of the American Institute of Electrical Engineers 71.1, 1952. Doi: [10.1109/AIEEPAS.1952.4498544](https://doi.org/10.1109/AIEEPAS.1952.4498544)

Kron, G. (7). [Tensorial Analysis of Integrated Transmission Systems; Part IV. La interconexión de los sistemas de transmisión](#). Power Apparatus and Systems. Transactions of the American Institute of Electrical Engineers 72.2, 1953. Doi: [10.1109/AIEEPAS.1953.4498707](https://doi.org/10.1109/AIEEPAS.1953.4498707)

Happ, H. H. [Diakoptics-The solution of system problems by tearing](#). Actas del IEEE 62.7, 1974. DOI: [10.1109/PROC.1974.9545](https://doi.org/10.1109/PROC.1974.9545)

Fundamentals

Chung-Wen, H.; Ruehli, A. & Brennan, P. [The modified nodal approach to network analysis](#). Circuits and Systems, IEEE Transactions on, 1975, vol. 22, no 6, pp. 504-509. DOI: [10.1109/TCS.1975.1084079](https://doi.org/10.1109/TCS.1975.1084079)

Linares, L. R. & Martí, J. R. [Sub-area latency in a real time power network simulator](#). International Conference on Power System Transients, 1995, pp. 541-545.

Supports

Dommel, H. W. [Programa de transitorios electromagnéticos: Manual de referencia](#). Bonneville Power Administration, 1986.

Martí, J. R. (1); Linares, L. R.; Calvino, J. & Dommel, H. W. [OVNI: An Object Approach to Real-Time Power System Simulators](#). Power System Technology, 1998. Actas. POWERCON'98. Conferencia internacional de 1998. Vol. 2. IEEE, 1998, pp. 977-981. **DOI:** [10.1109/ICPST.1998.729230](https://doi.org/10.1109/ICPST.1998.729230)

Martí, J. R. (2); Linares, L. R.; Hollman, J. A. & Moreira, F. A. [OVNI: Integrated software/hardware solution for real-time simulation of large power systems](#). Actas del PSCC. Vol. 2. 2002.

Moreira, F. A. (2); Martí, J. R. & Zanetta Jr, L. C. [Multirate Simulations With Simultaneous-Solution Using Direct Integration Methods in a Partioned Network Enviroment](#). 2006, pp. 2765-2777. **DOI:** [10.1109/TCSI.2006.882821](https://doi.org/10.1109/TCSI.2006.882821)

Moreira, F. A. (3) & Martí, J. R. [Latency techniques for time-domain power system transients simulation](#). Power Systems, IEEE Transactions on 20, no. 1, 2005, pp 246-253. **DOI:** [10.1109/TPWRS.2004.841223](https://doi.org/10.1109/TPWRS.2004.841223)

Tomim, M. A. (1); Martí, J. R.; De Rybel, T.; Wang, L. & Yao, M. [MATE network tearing techniques for multiprocessor solution of large power system networks](#). Power and Energy Society General Meeting, 2010 IEEE. IEEE, 2010, pp. 1-6. **DOI:** [10.1109/PES.2010.5590110](https://doi.org/10.1109/PES.2010.5590110)

Tomim, M. A. (2); De Rybel, T. & Martí, J. R. [Extending the Multi-Area Thévenin Equivalents method for parallel solutions of bulk power systems](#). International Journal of Electrical Power & Energy Systems, 2013, vol. 44, no 1. <https://doi.org/10.1016/j.ijepes.2012.07.037>

Tomim, M. A. (3); Martí, J. R. & Wang, L. [Parallel solution of large power system networks using the Multi-Area Thévenin Equivalents \(MATE\) algorithm](#). International Journal of Electrical Power & Energy Systems 31, 2009. <https://doi.org/10.1016/j.ijepes.2009.02.002>

Differences

Moreira, F. A. (1); Martí, J. R. & Linares, L. R. [Electromagnetic transients simulation with different time steps-The latency approach](#). Proc. Int. Conf. Power System Transients (IPST), New Orleans, USA. 2003.

Semlyen, A. & De Leon, F. [Computation of electromagnetic transients using dual or multiple time steps](#). Power Systems, IEEE Transactions on, 1993, vol. 8, no 3, pp. 1274-1281. **DOI:** [10.1109/59.260867](https://doi.org/10.1109/59.260867)

Vaidyanathan, P. P. [Multirate digital filters, filter banks, polyphase networks, and applications: A tutorial](#). Actas del IEEE 78.1, 1990, pp. 56-93. **DOI:** [10.1109/5.52200](https://doi.org/10.1109/5.52200)

Venerdini, G. (2); Guidi, D.; Zini, H. C. & Rattá, G. [Two-channel multirate network equivalent aimed to real-time electromagnetic transient calculation](#). Generation, Transmission & Distribution, IET, 2012, vol. 6, no 8, pp. 738-750. **DOI:** [10.1049/iet-gtd.2011.0827](https://doi.org/10.1049/iet-gtd.2011.0827)

Zini, H. & Ratta, G. [Multirate modeling scheme for electromagnetic transients calculation](#). Power Delivery, IEEE Transactions on, 2004, vol. 19, no 1. **DOI:** [10.1109/TPWRD.2003.817745](https://doi.org/10.1109/TPWRD.2003.817745)

Debates

Davidson, D. B.: [«A parallel processing tutorial](#). Antennas and Propagation Magazine, IEEE, 1990, vol. 32, no 2, pp. 6-19. **DOI:** [10.1109/74.80494](https://doi.org/10.1109/74.80494)

Martí, J. R. (3). [Accurate Modeling of Frequency Dependent Transmission Lines in Electromagnetic Transient Simulations](#). IEEE Trans. on PAS, vol. PAS-101, pp. 147-157, 1982. **DOI:** [10.1109/TPAS.1982.317332](https://doi.org/10.1109/TPAS.1982.317332)

Morched, A.; Gustavsen, B. & Tartibi, M. [A universal model for accurate calculation of electromagnetic transients on overhead lines and underground cables](#). Power Delivery, IEEE Transactions on, 1999, vol. 14, no 3, pp. 1032-1038. **DOI:** [10.1109/61.772350](https://doi.org/10.1109/61.772350)

Naredo J. L. (1); Soudack, A. & Martí, J. R. [Simulación de transitorios en líneas de transmisión con corona mediante el método de las características](#). Generation, Transmission and Distribution, IEE Proceedings-IET, 1995. pp. 81-87. **DOI:** [10.1049/ip-gtd:19951488](https://doi.org/10.1049/ip-gtd:19951488)

Naredo, J. L. (2); Mahseredjian, J., Kocar, I.; Gutiérrez-Robles, J. A. & Martínez-Velasco, J. A. [Frequency Domain Aspects of Electromagnetic Transient Analysis of Power Systems](#). IEEE/PES Tutorial on Electromagnetic Transients in Power Systems. Solution Techniques, Applications, Simulation Tool Development, Editor: J. A. Martínez-Velasco, pp. 20-36. **DOI:** [10.1002/9781118694190.ch3](https://doi.org/10.1002/9781118694190.ch3)

Venerdini, G. (1); Guidi, D.; Zini, H. C.; Rattá, G. & Arispe, J. C. G. [Multirate network equivalent model for electromagnetic transient calculation in real time](#). Conferencia y Exposición de Transmisión y Distribución: Latinoamérica (T&D-LA), 2010 IEEE/PES. IEEE, 2010. pp. 155-162. **DOI:** [10.1109/TDC-LA.2010.5762876](https://doi.org/10.1109/TDC-LA.2010.5762876)